

NASA TM X-55854

CALCULATION OF SIGNAL MARGINS FOR THE CSM UNIFIED S-BAND DOWNLINK CHANNEL APOLLO AS-202 TO AIRCRAFT NASA 432

GPO PRICE \$ _____

CFSTI PRICE(S) \$ _____

Hard copy (HC) 3.00

Microfiche (MF) .65

653 July 65

FACILITY FORM 602

N67-33855
(ACCESSION NUMBER)

33
(PAGES)

(NASA CR OR TMX OR AD NUMBER)

(THRU) _____

COPY

07
(CATEGORY)

AUGUST 1966



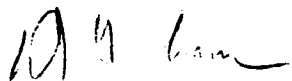
GODDARD SPACE FLIGHT CENTER
GREENBELT, MARYLAND

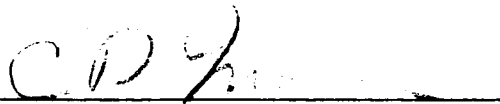
**CALCULATION OF SIGNAL MARGINS
FOR THE CSM
UNIFIED S-BAND DOWNLINK CHANNEL
APOLLO AS-202 TO AIRCRAFT NASA 432**

August 1966

Prepared by

David A. Dalglish, Chairman
Electronic-Electrical Engineering Technology
Spring Garden Institute
Philadelphia, Pennsylvania
NASA-ASEE Faculty Fellow

Review by 
D. J. Graham
Instrumented Aircraft Section

Approved by 
C. D. Mason
Head, Instrumented Aircraft Section

**GODDARD SPACE FLIGHT CENTER
GREENBELT, MARYLAND**

CONTENTS

<u>Section</u>	<u>Title</u>	<u>Page</u>
1	CALCULATION OF SIGNAL MARGINS	1
1.1	Introduction and Limitations of Calculations	1
2	SUMMARY OF RESULTS	3
3	DETAIL CALCULATION PROCEDURES NOTES	8
3.1	General	8
3.2	Fixed Specified Parts of the Margin	8
3.2.1	Transmitter Output Power (P_t)	8
3.3.2	Transmitter Output Circuits Losses (L_{tc})	8
3.3.3	Time Variable Values	20
4	FUTURE WORK	27
5	ACKNOWLEDGEMENTS	28
6	REFERENCES	29

FIGURES

<u>Number</u>	<u>Title</u>	<u>Page</u>
1	Apollo 202 Entry Trajectory and Blackout Boundaries	2
2	CSM USB Downlink Channel Block Diagram	3
3	AS-202/NASA 432 USB Downlink Signal Margin Variations	7
4	Ellipse Orientation	12
5	AGC Recording of the Apollo AS-201/NASA 232 (2/26/66) Signal Strength in Minus dbm vs Time in Seconds	14
6	Total System Effective Noise Temperature Contributions	15
7	USB Frequency Spectrum	17
8	AS-202/NASA 432 USB Downlink Transmitting Antenna Gain vs Time	21
9	Propagation Plot of Apollo CM Model	22

FIGURES (Continued)

<u>Number</u>	<u>Title</u>	<u>Page</u>
10	Coordinate System	23
11	Apollo SCIN Antenna Location (View Looking Aft)	24
12	Spacecraft Coordinates in Reentry Attitude at Position 80 Seconds After Entry	25
13	Space Loss	26
14	Space Losses at 2287.5 Mc	28

TABLES

<u>Number</u>	<u>Title</u>	<u>Page</u>
1	Tracking/Acquisition Margin - 500-nmi Slant Range and Transmitter Power of 10.0 Watts at 2.2875 Gc	4
2	Data Margin - 100-nmi Slant Range and Transmitter Power of 10.0 Watts at 2.2875 Gc and with PCM/PM/PM TLM on 1.024-Mc Subcarrier at a 51.2 kbps Rate	5
3	Margin Variations due to Space Loss and Transmitting Antenna Gain Tracking, Fixed Level -165.4 dbw (Data is 14 db Below Tracking Margin)	6

1. CALCULATION OF SIGNAL MARGINS

1.1 INTRODUCTION AND LIMITATIONS OF CALCULATIONS

Margin determinations have been done many times in the past for both communications and radar channels. Calculations have already been completed for equipment in part of the Apollo program, Apollo/Range Instrumentation Aircraft (A/RIA) (ref. 1). It is the purpose of this report to accumulate in one place the various details involved in margin determinations and, at the same time, to give an illustration of the use of these details.

The practical parts of this determination will involve the Apollo AS-202 mission. During re-entry phase of this mission, the effects of plasma interference (blackout) on the command and service module's (CSM) unified S-band (USB) downlink communications channel to an aircraft is to be investigated. The general thought is that a signal from the spacecraft may be distinguishable if a receiver was located in such a position behind the spacecraft as it re-enters the earth's atmosphere and goes into the "blackout" region. That emission would be viewed in the angle between the plasma sheath in front and the ionized trail behind.

The aircraft for the experiment is a C-54, designated NASA 432. The spacecraft transmission, as specified for the Block I Saturn-Apollo vehicle, is at a carrier frequency of 2.2875 Gc with two subcarriers: telemetry (TLM) at a 51.2 thousand bits per second (kbps) rate on 1.024 Mc (PCM/PM/PM), voice on 1.25 Mc (FM/PM). The aircraft will be using a DEI Model TTR-1 tracking receiver having a 500-kc and a 20-kc bandwidth, and a Vitro Electronics Model 1037E data baseband receiver having a 3.3-Mc bandwidth phase demodulator (PTD 113A) with the A/RIA data demodulator.

This determination of signal margins does not contain any anticipated losses due to plasma interference, additional attenuation in space due to the proximity of other bodies, or the losses due to multipath when the spacecraft is only a few degrees above the horizon. The calculations are all based on the latest information on the spacecraft trajectory as of August 11, 1966. This information shows the spacecraft re-entry at 4.62 degrees south latitude and 136.36 degrees east longitude and at an altitude of 400,000 feet (see figure 1).

The blackout point is not, and can not, be as accurately defined. It is anticipated that blackout will occur approximately 100 ± 10 seconds after re-entry.

The aircraft is to be located over Vanimo, Australian administrated New Guinea (2.7 degrees south latitude, 141.3 degrees east longitude); and, as far as these calculations are concerned, it is assumed to be in a fixed position.

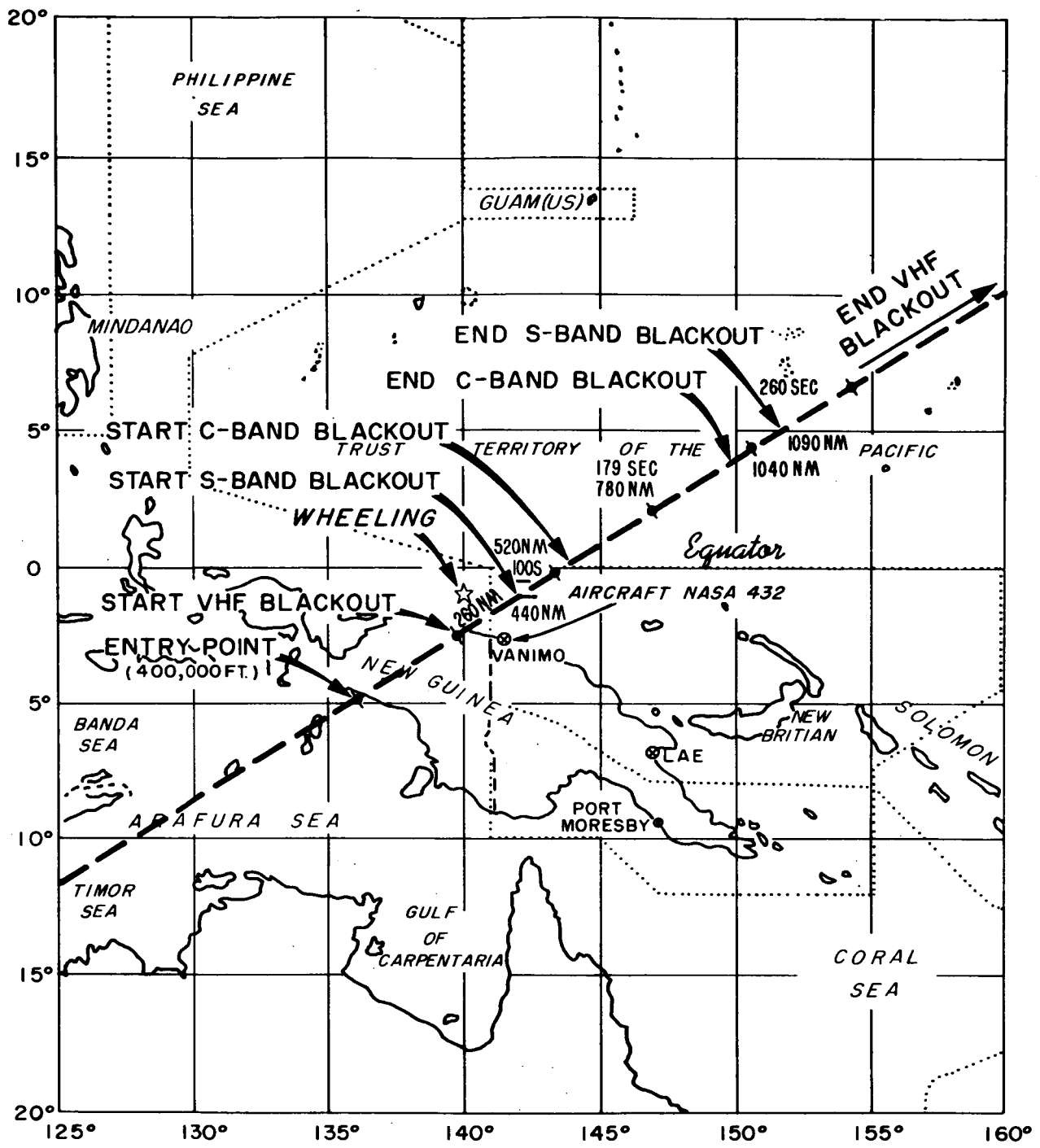


Figure 1. Apollo 202 Entry Trajectory and Blackout Boundaries (See Reference 8)

2. SUMMARY OF RESULTS

The system for which this signal margin was determined is illustrated in figure 2. The definition of the symbols are found in the tabulated results of this study, table 1 and table 2. This margin determination includes two parts, consisting of tracking and data. In both cases acquisition is considered in the summary, at 500-nmi slant range for tracking acquisition and at 100-nmi slant range for data acquisition. The results of the calculations for signal margins are given in table 1, tracking; table 2, data; and figure 3. For both sets of calculations, a "most likely" value and a "maximum" value was determined. In all cases, a USB power level of 10 watts (10 dbw) is used. The various parameters used in these calculations are justified in notes in the last part of this report and are referenced in table 1 and 2.

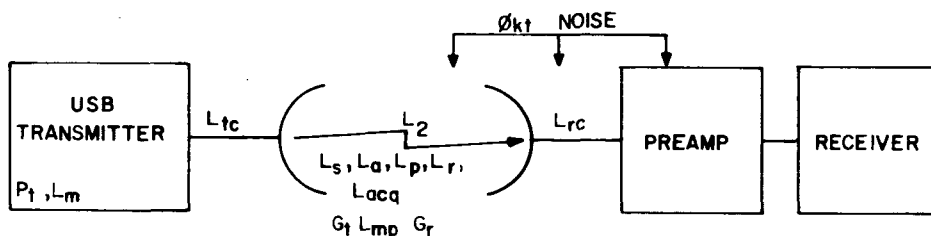


Figure 2. CMS USB Downlink Channel Block Diagram

For the tracking mode (table 1) with the spacecraft at 500 nmi, the signal margin is +0.4 db based on the measured value of received power required for good tracking of full power, carrier and sideband, of -116 dbm. Tracking acquisition should occur at -49 seconds (550 nmi slant range). No noise tracking error analysis was performed for the data margins (TLM and voice), with the spacecraft at 100 nmi and the margin is +0.4 db for the 51.2-kbps data rate (table 2). Data acquisition should occur at approximately +60 seconds (100-nmi slant range). These data margins are based on a bit error probability of 10^{-2} . It is found that the carrier (tracking) margin is 14 db higher than the data (TLM) margin.

The variations in both margins with time; also slant range and ground range, are shown in figure 3. The deep dips in the plot are caused by rapid changes in the transmitting antenna gains. To observe the results of entering the blackout region it would be best if blackout does not occur at a time when the signal strength is in a trough. It is also possible that acquisition will not occur at the 550-nmi slant range indicated in figure 3 because at that low angle, close to the horizon, multipath may cause momentary reductions in the signal. Best results will be seen if blackout occurs after -100 seconds because in this condition the only variable is the space loss and it only increases slowly, at a rate of 6 db/100 miles.

The details of the tabulations that went into figure 3 are shown in table 3.

Table 1. Tracking/Acquisition Margin - 500-nmi Slant Range and Transmitter Power of 10.0 Watts (10 dbw) at 2.2875 Gc

Item	Reference Paragraph	Worst Case Value	Most Likely Value
1 P_t , transmitter power (10.0 watts nominal)	3.2.1	10.0 dbw	10.0 dbw
2 L_{tc} , transmitter output circuit losses	3.2.2	-7.0 db	-5.6 db
3 G_t , transmitting antenna gain	3.3.2.13	-9.0 db	-6.0 db
4 L_2 , losses between antennas		-167.5 db	-167.5 db
(a) L_s , space losses (500 nmi)	3.3.3.2		
(b) L_a , atmospheric attenuation	3.3.2.2		
(c) L_p , polarization losses	3.3.2.3		
(d) L_r , radome losses	3.3.2.4		
(e) L_{acq} , scanning beam loss	3.3.2.5		
5 G_r , receiving antenna gain	3.3.2.8	+24.0 db	+24.0 db
6 L_{rc} , receiving antenna circuit losses	3.3.2.9	-0.45 db	-0.45 db
7 P_r , totals for signal (gains - losses)		-150.0 db	-145.55 db
(a) Gains: $P_t + G_t + G_r = [10 + (-6) + 24] = +28$ db			
(b) Losses: $L_{tc} + L_2 + L_{rc} = 5.6 + 167.5 + .45 = 173.55$			
8 Measured full power, carrier and sideband, required for acceptable antenna tracking	3.3.2.12	-146.0 dbw	-146.0 dbw
9 Margin		-4.0 db	+0.45 db

Table 2. Data Margin - 100-nmi Slant Range and Transmitter Power of 10.0 Watts at 2.2875 Gc and with PCM/PM/PM TLM on 1.024-Mc Subcarrier at a 51.2 kbps Rate

	Items	Reference Paragraph	Worst Case Value	Most Likely Value
1	P_t , transmitter power (10.0 watts, nominal)	3.2.1	+10.0 dbw	+10.0 dbw
2	L_m , subcarrier modulation losses	3.3.2.1	-7.86 db	-5.17 db
3	L_{tc} , transmitter output circuit losses	3.2.2	-7.0 db	-5.6 db
4	G_t , transmitting antenna gain	3.3.2.13	-9.0 db	-6.0 db
5	L_2 , losses between antennas			
	(a) L_s , space loss (100 nmi) -144.6 db	3.3.3.2	-151.4 db	-151.4 db
	(b) L_a , atmospheric attenuation -2.0 db	3.3.2.2		
	(c) L_p , polarization losses -3.0 db	3.3.2.3		
	(d) L_r , radome losses -0.5 db	3.3.2.4		
	(e) L_{pt} , antenna pointing loss - 1.25 db	3.3.2.6		
	(f) L_{mp} , loss due to multipath 0.0 db	3.3.2.7		
6	G_r , receiver antenna gain	3.3.2.8	+24.0 db	+24.0 db
7	L_{rc} , receiving antenna circuit losses	3.3.2.9	-0.45 db	-0.45 db
8	P_r , totals for signal (gains - losses)		-141.7 db	-134.6 db
	(a) Gains: $P_t + G_t + G_r = [10 + (-6) + 24] = +28$ db			
	(b) Losses: $L_m + L_{tc} + L_2 + L_{rc} = 5.17 + 5.6 + 151.4 + .45 = -162.62$			
9	ϕ_{kt} , noise spectral density, $T_{sys} = 643.1^\circ K$	3.3.2.10	-201.24 db/cycle	-201.24 db/cycle
10	Bandwidth (462 kc) predetection		+56.64	+56.64
11	$(S/N)_{db}$, predetection	3.3.2.11	+2.9 db	+10.0 db
12	$(S/N)_{db}$, postdetection	3.3.2.11	+0.9 db	+8.0 db
13	$(S/N)_{db}$, 10^{-4} bit error rate	3.3.2.12	+7.6 db	+7.6 db
14	Margin		-6.7 db	+0.4 db

Table 3. Margin Variations due to Space Loss and Transmitting Antenna Gain
Tracking, Fixed Level -165.4 dbw (Data is 14db Below Tracking Margin)

Time (sec) Position	Slant (nm) Range	Approx. Ground Range (nm) (Spacecraft)	Altitude (k ft)	Bank Angle (degree)	ϕ (degree)	θ (degree)	Time Variant Losses		Tracking Margin (db)	
							Space Loss (db)	Antenna Gain Gt (db)		
-195	1182.8		866.5	+180	5.9	148.2	-166.3	-6	-6.9	
-159	1028.4		763.1	+180	7.0	148.8	-165.0	-6	-6.4	
-126	883.4		673.4	+180	8.3	149.3	-163.6	-6	-4.2	
-106	796.5		623.0	+180	9.3	149.6	-162.8	-6	-3.4	
-86	708.8		575.3	+180	10.4	149.7	-161.6	-6	-2.2	
-60	595.1		517.1	+180	12.6	149.7	-160.0	-6	-0.6	
Horizon	550.0			+180			-159.4	-6	0.0	
-42	516.0		479.4	+180	14.3	149.5	-159.1	-6	+0.3	
	500.0			+180			-159.0	-6	+0.4	
-26	446.2		447.9	+180	16.4	149.1	-158.0	-6	+1.4	
Entry	0	0	400.0	+180	20.9	147.7	-155.2	<-6	+4.2	
12	281.0	52.8	379.7	+180	23.7	146.4	-154.0	<-6	+5.4	
20	247.3	87.8	366.7	+180	26.1	145.1	-152.7	<-6	+6.7	
32	197.5	140.7	348.0	+180	30.3	142.2	-150.7	<-12	+2.7	
40	165.9	175.8	336.2	+180	33.8	139.0	-149.3	<-15	+1.1	
46				+180			~-147.9	-15 *	+2.5	
52	122.1	228.6	319.2	+180	40.3	130.0	-146.5	-12	+6.9	
53	120			+180			-146.1	~-11	+7.3	
56				+180			-145.7	<-6 *	+13.7	
59	100			+180			-144.6	<-6 *	+14.4	
60	98.2	264.2	308.5	+180	45.8	117.0	-144.5	-9	+11.9	
61				+180			-144.3	<-6 *	+15.1	
63				+180	48.0	105.0	-144.0	-3 *	+18.4	
66				+180	51.0	93.0	-143.7	<-3 *	+18.7	
68	83.99			+180	52.6	90.0				
69				+180	54.0	81.0	-143.4	<-3 *	+19.0	
Min. offset 66 nm	72	81.6	317.4	293.3	+180	56.4	69.5	-143.0	<-3	+19.4
74				+180			~-143.1	<-3 *	+19.3	
76				+180	60.5	49.1	~-143.2	-9 *	+13.2	
77				+180			~-143.2	-15 *	+7.2	
78				+180			~-143.3	<-15 *	+7.1	
80	85.5	352.5	283.7	+180	64.8	32.3	-143.4	<-9	+13.0	
84				+180	69.5	20.6				
92	120.2	405.8	270.2	+180	79.8	6.9	-146.3	<-3	+16.1	
94	126.8			+171	72.8	9.2	-146.9	<-3	+15.5	
95.5				163 @ 95 sec			-147.3	<-18	+6.1	
S-band Blackout	96	133.8		+135	19.3	15.8	-147.6	<-3	+14.8	
	98	140.7		110 @ 97 sec 92	293.7	8.8	-147.9	<-15	+5.5	
	98.5			68 @ 99 sec				-15		
100	148.3	441.4	261.6	+50.0	250.7	13.0	-148.3	<-3	+14.1	
104	163.2	458.7	257.4	-5.0	210.8	43.4	-149.2	-3	+13.2	
112		494.6		-4.0	208.2	39.3				
120	228.0	529.4	242.3	-2.5	206.2	36.5	-152.0	<-3	+10.4	
140	311.4		227.9	+10.0	206.2	30.2	-154.9	<-3	+7.5	
160	395.7		219.4	+31.0	208.5	24.6	-156.8	<-3	+5.6	
180	477.3	785.7	217.3	-39.0	184.3	34.2	-158.5	<-3	+3.9	
200	558.1		219.7	-52.0	175.7	31.6	-159.7	<-3	+2.7	
220	635.9		224.7	-53.0	174.0	30.7	-160.6	<-3	+1.8	
End	240	713.3	1022.0	231.1	-43.0	175.6	30.7	-161.6	<-3	+0.8
Blackout	260	788.5	1090.0	238.1	-42.5	174.4	30.7	-162.8	<-3	-0.4
Horizon	280	862.8	245.2	-42.0	173.3	30.8	-163.3	<-3	-0.9	
300	936.5	1246.0	251.6	-41.0	172.5	31.1	-164.1	<-3	-1.7	

*Interpolated points

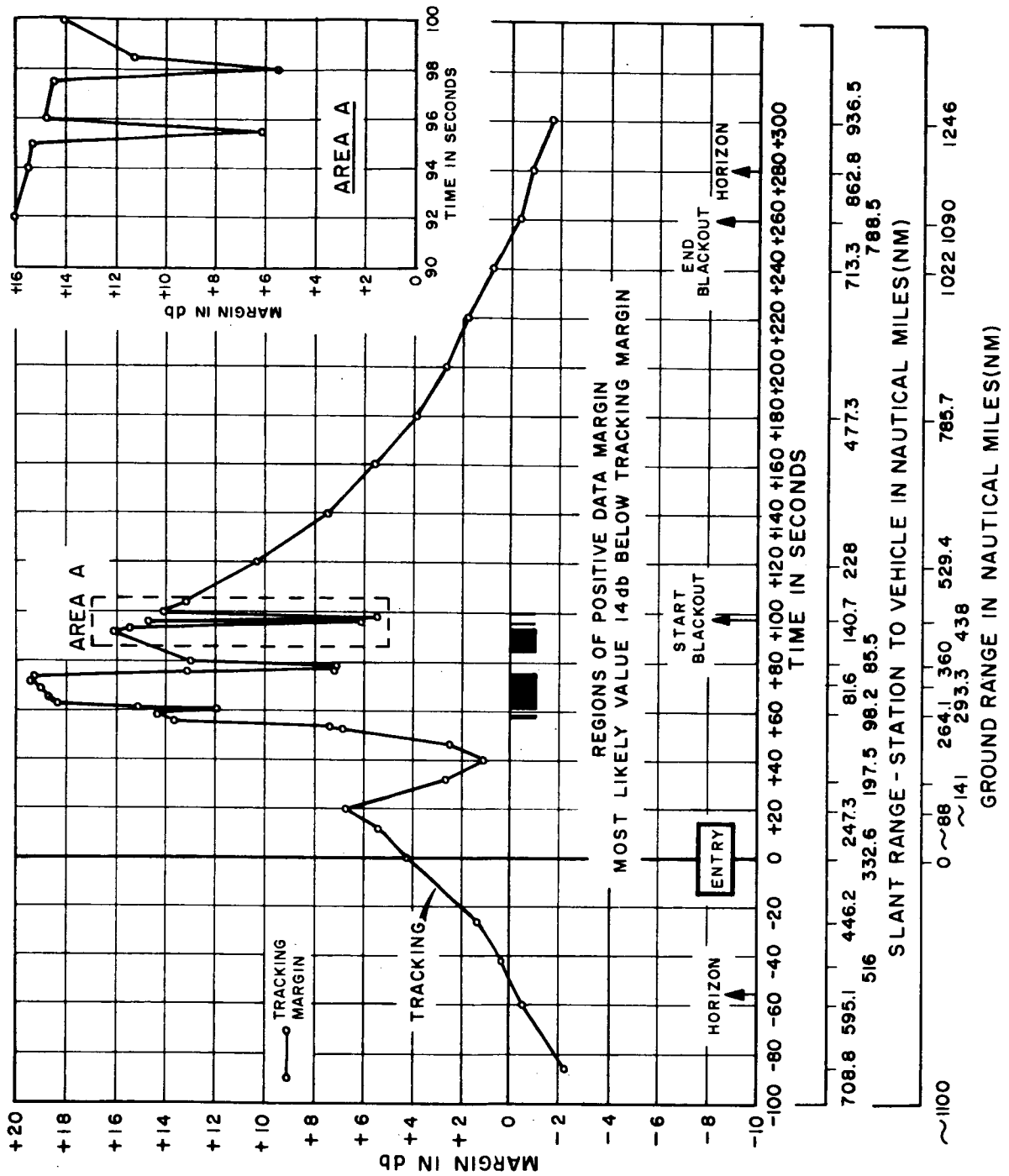


Figure 3. AS-202/NASA 432 USB Downlink Signal Margin Variations

3. DETAIL CALCULATION PROCEDURES NOTES

3.1 GENERAL

Since the accuracy of a signal margin determination can only be as accurate as the parts that make it up, it is the expressed purpose of this phase of the report to identify and verify each part of the calculations. When properly presented, mistakes can be easily spotted and corrected; one small part at a time.

Two major parts exist in the calculations: fixed given specifications and calculated parts of the margin. The last part also has two basic areas, fixed values and time variable values.

3.2 FIXED SPECIFIED PARTS OF THE MARGIN

This information should be obtained from the specifications of the spacecraft and/or other specifications for the particular mission involved.

3.2.1 TRANSMITTER OUTPUT POWER (P_t)

According to the Ground Operational Support System Interface Report, Section I, the Apollo Spacecraft, North American Aviation, Inc., SID 63-881, reissued 15 February 1964, page 391; and S-Band Power Amplifier Equipment, North American Aviation, Inc. Specification MC478-0020A, Amendment 1 dated 29 July 1963; the CSM transmitter power levels assumed throughout early studies were:

High Power:	14.4 watts	+11.58 dbw (41.58 dbm)
Low Power:	2.9 watts	+ 4.62 dbw (34.62 dbm)

However, from later reports it seems that 10 watts (10 dbw or 40 dbm) is a more likely value.

It is necessary to obtain an expression of absolute power level using the decibel notation. A standard reference level of power is 1 mw; and using this reference, power can be expressed as a number of dbm above (+) or below (-) 1 mw. Another reference is 1 watt, and this will allow a power to be expressed as a number of dbw above or below 1 watt. Both references will be used.

3.2.2 TRANSMITTER OUTPUT CIRCUITS LOSSES (L_{tc})

From the CSM - MSFN signal performance and interface specification for Block I, losses are specified as 7 db; but, using information from later reports, 5.6 db seems to be a more likely figure.

3.3 CALCULATED PARTS OF THE MARGIN

3.3.1 GENERAL

Most of the fixed and variable parts of the calculations have several good references. Some of the better ones are indicated on the reference page. In general, this part is a collection of nonoriginal work used for this specific mission.

3.3.2 FIXED VALUES

Fixed values are those that do not vary with time during the mission. This does not mean that they cannot vary due to other influences.

3.3.2.1 Subcarrier Modulation Losses (L_m)

The PM indices for modulation of the USB carrier by the voice and TLM subcarriers for Block I are specified as:

TLM Data Rate	Subcarrier	Phase Modulation Index (Radians Peak)
51.2 kbps	Voice 1.25 Mc (FM/PM)	$0.84 \pm 0.12 (\Delta\theta_1)$
	TLM 1.024 Mc (PCM/PM/PM)	$1.1 \pm 0.185 (\Delta\theta_2)$

In reference 2, Walch derives the formulas used in determining the ratios of the total power transmitted that remains in the carrier channel or each subcarrier channel for a system with frequency, or phase modulated signals, modulated by a number of subcarriers. This is accomplished with trigonometric identities and Bessel Function identities. The results show that if the total power, P_t , in the transmitted wave is proportional to E_c^2 (E_c being carrier voltage), then the total power, P_c , transmitted at the carrier frequency is proportional to:

$$[J_0(M_1)J_0(M_2)\dots J_0(M_n)E_c]^2$$

$$\text{and } \frac{P_c}{P_t} = [J_0(M_1)J_0(M_2)\dots J_0(M_n)]^2$$

$$\text{which leads to } \frac{P_c}{P_t} = \left[\prod_{i=1}^n J_0(M_i) \right]^2$$

where: M_i = modulating factor for each subcarrier

n = number of subcarriers

For two subcarriers (phase modulated) this equation becomes

$$\frac{P_c}{P_t} = [J_0(\Delta\theta_1)J_0(\Delta\theta_2)]^2$$

Now, if the total power, P_t , in the transmitted wave is again proportional to E_c^2 , then the total power, P_{sc} , transmitted at the subcarrier frequency, W_i , is proportional to:

$$2[J_0(M_1)J_0(M_2)\dots J_0(M_j)J_1(M_i)E_c]^2$$

$$\text{and } \frac{P_{sc}(W_i)}{P_t} = 2 [J_0(M_1)J_0(M_2)\dots J_0(M_j)J_1(M_i)]^2$$

$$\text{can be written as } \frac{P_{sc}(W_i)}{P_t} = 2 \left[\prod_{j, i=1}^n J_0(M_j)J_1(M_i) \right]^2$$

where: $j \neq i$

n = number of subcarriers

j = subcarrier being considered

M_i = modulating factor or index

By combining equations (3) and (6), the ratio of $P_{sc}(W_i)$ to P_t can be found in relation to P_c/P_t .

$$\frac{P_{sc}(W_i)}{P_t} = 2 \frac{P_c}{P_t} \left[\frac{P_c J_1(M_i)}{P_t J_0(M_i)} \right]^2$$

To complete the calculations of the modulation losses, the following Bessel functions have been obtained using a four place table.

a. Voice

$$\Delta\theta_1 = 0.84 \pm 0.12$$

$$J_0(\Delta\theta_1) = J_0(0.84 \pm 0.12) = .8308 \begin{cases} J_0(.96) = .7821 \\ J_0(.72) = .8742 \end{cases}$$

$$J_1(\Delta\theta_1) = J_1(0.84 \pm 0.12) = .3836 \begin{cases} J_1(.96) = .4263 \\ J_1(.72) = .3370 \end{cases}$$

b. TLM

$$\Delta\theta_2 = 1.1 \pm .185$$

$$J_0(\Delta\theta_2) = J_0(1.1 \pm .185) = .7196 \begin{cases} J_0(1.285) = .6277 \\ J_0(.915) = .8012 \end{cases}$$

$$J_1(\Delta\theta_2) = J_1(1.1 \pm .185) = .4709 \begin{cases} J_1(1.285) = .5184 \\ J_1(.915) = .4064 \end{cases}$$

As a check, the rms index should be near $1 \pm .2$.

$$\begin{aligned} \text{RMS Index} &= \sqrt{\left(\frac{\Delta\theta_1}{\sqrt{2}}\right)^2 + \left(\frac{\Delta\theta_2}{\sqrt{2}}\right)^2} = \frac{1}{\sqrt{2}} \sqrt{(.84)^2 + (1.1)^2} \\ &= \frac{1}{\sqrt{2}} \sqrt{.706 + 1.21} = .707 \sqrt{1.916} = .972 \end{aligned}$$

The carrier modulation losses are:

$$\text{Most likely value: } \frac{P_c}{P_t} = [J_0(\Delta\theta_1) J_0(\Delta\theta_2)]^2 = [(.83) (.7196)]^2 = .357$$

$$10 \log \frac{P_c}{P_t} = 10 \log .357 = 10 (-\log 2.8) = -4.5 \text{ db}$$

$$\text{Maximum value: } \frac{P_c}{P_t} = [J_{0m}(\Delta\theta_1) J_{0m}(\Delta\theta_2)]^2 = [(.7821) (.6277)]^2 = (.49)^2 = .24$$

$$10 \log P_c/P_t = 10 \log .24 = 10 (-\log 4.17) = 10 (-.62) = -6.2 \text{ db}$$

The TLM subcarrier modulation losses are:

Most likely value:
$$\frac{P_{sc(TLM)}}{P_t} = 2 \frac{P_c}{P_t} \left[\frac{J_1(\Delta\theta_2)}{J_0(\Delta\theta_2)} \right]^2 = 2(.357) \left[\frac{(.4709)}{(.7196)} \right]^2 = .305$$

$$10 \log \left(\frac{P_{sc(TLM)}}{P_t} \right) = 10 \log .305 = 10 (-\log 3.285) = \underline{\underline{-5.17 \text{ db}}}$$

Maximum value:
$$\frac{P_{sc(TLM)}}{P_t} = 2 \frac{P_{c_m}}{P_{t_m}} \left[\frac{J_{1_m}(\Delta\theta_2)}{J_{0_m}(\Delta\theta_2)} \right]^2 = 2(.24) \left[\frac{J_1(1.285)}{J_0(1.285)} \right]^2 = .1635$$

$$10 \log \left. \frac{P_{sc(TLM)}}{P_t} \right|_{\max} = 10 \log .1635 = 10 (-\log 6.12) = -7.86 \text{ db}$$

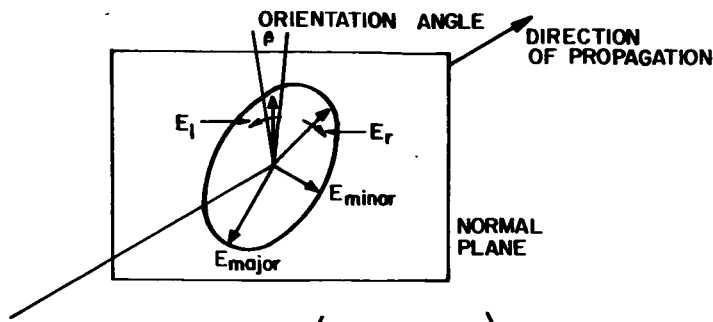
3.3.2.2 Atmospheric Attenuation (L_a). The atmospheric attenuation due to oxygen and water vapor at 2.3 Gc and zero elevation angle is -2.0 db (ref. 3 and 5).

3.3.2.3 Polarization Losses (L_p)

It is usually best in receiving a signal to use an antenna that has a polarization identical with that of the wave to be received. However, the spacecraft has a linearly polarized antenna and the aircraft has a circularly polarized antenna. Since the polarization of a radio wave is determined by the direction in which the electric vector is aligned during the passing of one complete cycle, if magnitude and pointing of the electric vector vary during a cycle, an ellipse will be mapped out in a plane normal to the direction of propagation. This is elliptical polarization. If the minor to major axis ratio is zero (ellipticity of infinite db), the polarization is linear; if the minor to major axis ratio is unity (ellipticity of 0 db), the polarization is circular.

For best transmission between two elliptically polarized antennas, three things are needed (ref. 9):

- a. Their axis ratio E minor/E major should be the same.
- b. Their predominant senses are the same.
- c. Their ellipse orientations are related by a minus sign:
B trans = -B received (see figure 4).



$$E_l = \frac{E_{\text{major}} \pm E_{\text{minor}}}{2}; E_r = \left(\frac{E_{\text{major}} \mp E_{\text{minor}}}{2} \right) e^{j2\beta}$$

ZERO PHASE DIFFERENCE BETWEEN E_r AND E_l WILL CAUSE E_{MAJOR} TO BE VERTICAL.

Figure 4. Ellipse Orientation

NOTE

For circular component synthesis of an elliptically polarized wave, see ref. 4, page 17-7.

When two antennas of different polarization are used, the normalized output power from the receiving antenna terminals are:

$$\frac{P}{P_{\text{max}}} = \frac{|(E_{r_1} E_{r_2} + E_{l_1} E_{l_2})|^2}{(E_{r_1}^2 + E_{l_1}^2)(E_{r_2}^2 + E_{l_2}^2)}$$

for this report, vertical antenna 1 (spacecraft) and circular antenna 2 (aircraft):

$$E_{r_1} = 1, E_{l_1} = 1e^{j0}, B = 0$$

$$E_{r_2} = 1, E_{l_2} = 0$$

$$\therefore \frac{P}{P_{\text{max}}} = \frac{|(1+0)|^2}{[1^2 + 1e^{j0}]^2} = 1/2$$

and

$$L_p = 10 \log \frac{P}{P_{\text{max}}} = 10 \log 1/2 = -3 \text{ db}$$

3.3.2.4 Radome Losses (L_r). The measured radome losses in NASA 432 aircraft is 0.5 db.

3.3.2.5 Scanning Beam Loss (L_{acq}). During acquisition scanning of the antenna beam, the diameter of the beam is taken as the 3 db points; therefore, a loss of 3 db is used as the losses due to acquiring the target at the edge of the scanning beam.

3.3.2.6 Antenna Pointing Loss (L_{pt}). Antenna pointing loss is based on a tracking error of about 2° in the NASA 432 human servo loop. Since the beamwidth of the antenna pattern is 7.8° at the half power (3 db) points, the antenna pointing loss would not be greater than 3 db. Assuming a linear change, a 2° error would give an approximate db loss of $10 \log 3/4$ or $-10 \log 4/3 = -1.25$ db.

3.3.2.7 Multipath Losses (L_{mp})

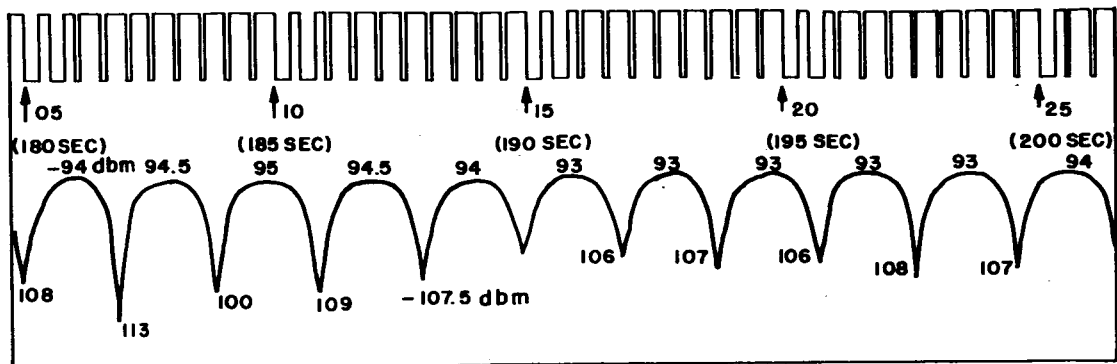
Multipath effects, as shown in figure 5, should be a very real part of data margin of a spacecraft to aircraft system, particularly when the spacecraft is at low elevation angles to the aircraft. Losses due to multipath can be as great as 30 db; and, since the effects vary with time, the only realistic method of handling multipath would be from a statistical point of view so as to be able to predict bit error.

The greatest losses occur at the lowest elevation angles, and these peak losses occur at approximately 2 to 3-second intervals. At a 51.2 kbps data rate, this would include 102.4 to 153.6 kilobits. At the range of about 540 nmi, for 10 percent of the time, the loss is greater than 10 db. If a 10-db average loss is used, this would mean that there would be at least 15,360 errors for every 153.6 kilobits. With this 10-db loss of figure, about 138,000 bits would get through without error (2.7 seconds of data) and 15,000 bits would be lost. Obviously, the bit error is enormous, suggesting that only the maximum loss can safely be used.

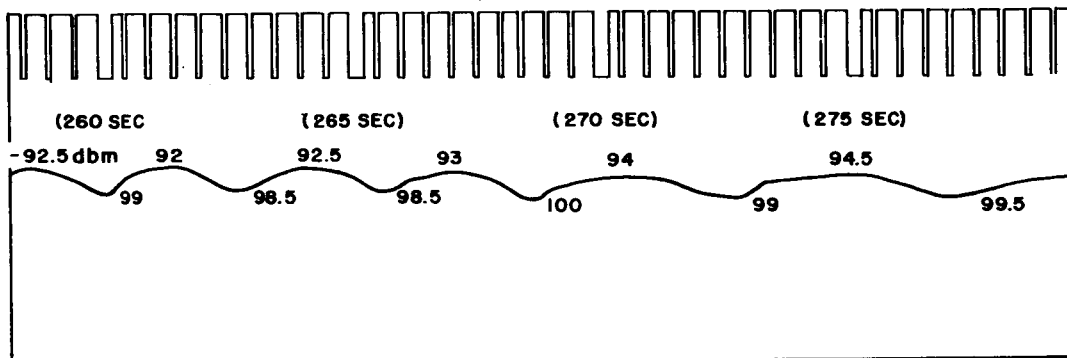
For the AS-202/NASA 432 mission, the data margin will be very bad at elevation angles near 3° since the range is great and the losses cause a negative margin. Therefore, this calculation is being made for short ranges of less than 200 nmi so that the margin will be slightly positive without considering multipath. The elevation angles at these ranges will exceed 10° , thereby effectively eliminating the multipath problem. For this reason multipath will not be included, but it should be remembered that should ranges of 500 nmi or greater be considered, multipath will introduce large additional errors.

3.3.2.8 Receiving Antenna Gain (G_r). The reference point for system noise calculations is usually taken at the antenna, ahead of the ohmic losses associated with feed components. For signal-to-noise calculations, the antenna gain should be referenced at the same point; and it is, therefore, important to determine the antenna gain value applicable at this point. The usual practice is to use the theoretical 100% efficiency gain and subtract the losses. These losses include spillover, aperture efficiency, and strut blockage. On the NASA 432, the S-band antenna is 4 feet and has a beamwidth at the -3 db points of 7.8° at 2.2875 Gc. The gain at the center of the beam is +24 db.

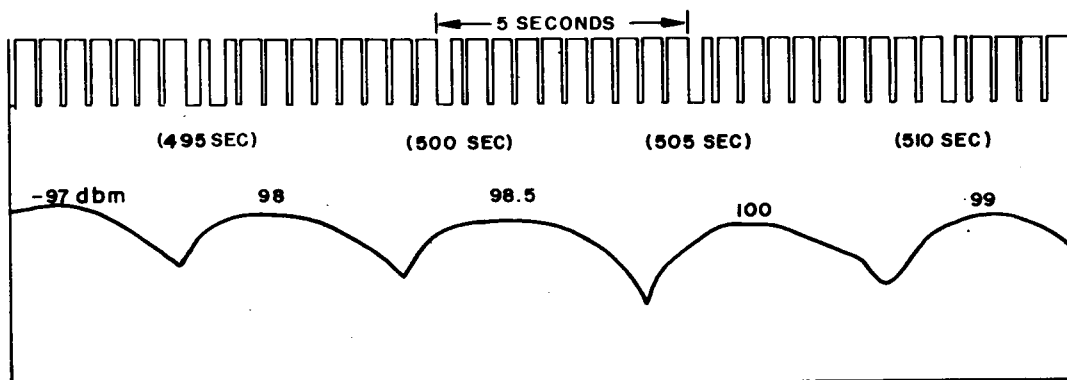
3.3.2.9 Receiving Antenna Circuit Losses (L_{rc}). The value of cabling losses for the receiving antenna was measured at -0.3 db. The losses of the coaxial switches used to disconnect the antenna from the tunnel diode preamplifiers is determined at -0.15 db. The total antenna circuit losses is then -0.45 db.



EL = +1° RANGE = 540 N.M



EL = +3.5° RANGE = 570 N.M.



EL = +2.5° RANGE = 750 N.M.

Figure 5. AGC Recording of the Apollo AS-201/NASA 232 (2/26/66)
Signal Strength in Minus dbm vs Time in Seconds

3.3.2.10 Noise Spectral Density (ϕ_{kt})

System noise temperature (T_{sys}) is required to obtain the noise spectral density. It is a combination of effective and actual temperatures; therefore it is sometimes referred to as total system effective noise temperature (ref. 5). Figure 6 shows the system noise temperature contributions.

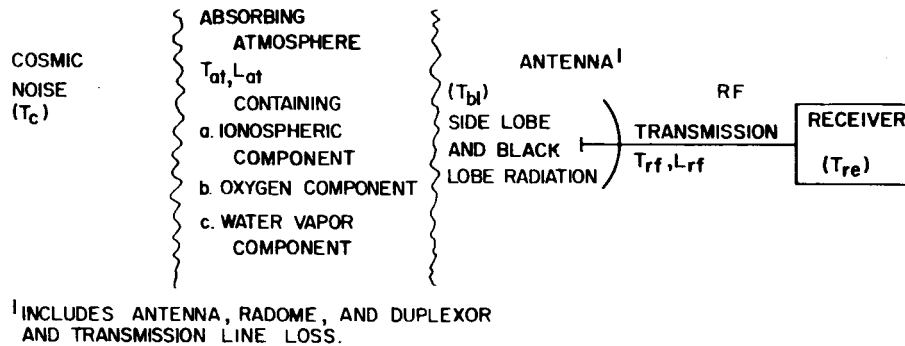


Figure 6. Total System Effective Noise Temperature Contributions

The equation for figure 6, showing the combining technique is:

$$T_e = T_1 + \frac{T_2}{G_1} + \frac{T_3}{G_1 G_2} + \dots + \frac{T_n}{G_1 G_2 \dots G_{n-1}}$$

Cosmic noise and atmospheric noise $[T_c + (L_{at} - 1) T_{at}]$ is called space temperature, brightness temperature, or the antenna temperature of an ideal antenna.

Assuming that the noise contributions enter the receiver via the main beam only, the effects of the side lobes may be neglected and:

$$T_e = T_c + (L_{at} - 1) T_{at} + (L_{rf} - 1) T_{rf} L_{at} + T_{re} L_{rf} L_{at}$$

assume: 1. $T_c + (L_{at} - 1) T_{at} = 103^\circ K$

2. $L_{rf} \alpha .3 \text{ db} \therefore .3 \text{ db} = 10 \log\left(\frac{\text{rf out}}{\text{rf in}}\right)$

$$\frac{\text{rf out}}{\text{rf in}} = \text{ant. log } .03 = 1.072$$

3. $T_{rf} \approx T_0 = 290^\circ K$

4. $L_{at} \alpha 1 \text{ db} \therefore 1 \text{ db} = 10 \log(L_{at} \text{ ratio})$

$$L_{at} \text{ ratio} = \text{ant. log } .1 = 1.105$$

$$5. F_{re} = 2.22 \text{ (see para 3.3.2.11)}$$

$$T_{re} = (F-1) T_o = (2.22 - 1)290$$

$$T_{re} = (1.22)290 = 355^\circ$$

then: $T_e = 103^\circ \text{ K} + (1.072 - 1)290^\circ \text{ K}(1.105) + 355^\circ \text{ K}(1.072) (1.105)$

$$T_e = 103^\circ \text{ K} + 23.1^\circ + 419^\circ + 545.1^\circ \text{ K}$$

finally: $\phi_{kt} = \text{Spectral Noise Density} = 10 \log (1.38 \times 10^{-23} \times 545.1^\circ \text{ K})$

$$\phi_{kt} = 10 \log (7.51 \times 10^{-21}) = 10(.876 - 21) = 10(-20.124)$$

$$\phi_{kt} = -201.24 \text{ db/cycle}$$

Using the narrow-band mode at a 20-kc bandwidth during tracking, the correction would be:

$$10 \log 20,000 = 10 (4.3) = +43 \text{ db}$$

For data margin calculations, a predetection noise bandwidth of 462 kc exists for the A/RIA demodulators:

$$10 \log 462,000 = 10 (5.664) = +56.64$$

3.3.2.11 Signal-to-Noise Ratio (S/N) for Bit Error Probability of 10^{-4}

The available S/N at this point is for the predetection (to 2nd detector) location. The predetection signal bandwidth in the data demodulator (A/RIA) is 384 kc (noise bandwidth is 462 kc), and the postdetection signal bandwidth is 75 kc (noise bandwidth is 90 kc).

There are two reasons for a change in the S/N as you go through the detector (predetection to postdetection). First, is the bandwidth improvement:

$$S/N_{\text{Postdet}} = S/N_{\text{Predet}} + 10 \log \frac{BW_{\text{if}}}{BW_{\text{Postdet}}}$$

$$\text{The improvement is} = 10 \log \frac{462 \text{ kc}}{2(90 \text{ kc})} = 10 \log 2.57 = +4.09 \text{ db}$$

Second, there is the change in S/N due to the modulation index. The basic equation for this is $[20 \log \sqrt{3} m_f]$ for frequency modulation. However, the TLM is phase modulated (actually biphas modulated). The modulation index is 1.1 ± 0.185 on the 1.024-Mc sub-carrier. Since the data demodulator is that of the A/RIA project, reference 1 is used as an information source. However, there seems to be some question as to the claims of phase-locked loop's system threshold improvement over zero-crossing detectors. The best way seems to be by actual measurement and not by analytic methods.

If the procedure used in reference 1 is used, with parameters from reference 6, it would first have to be noted that the carrier phase modulation index for TLM is 1.1 radians on the 51.2-kbps rate and the bandwidth is 3.3 Mc (IF's at 3 db). Actually, the voice subcarrier of 1.25 Mc determines the upper bandwidth limit.

$$BW = 2(\Delta F + F_m) + 2(7.5 \text{ kc} + 3 \text{ kc}) = 21 \text{ kc}$$

where: ΔF is the subcarrier's peak deviation
 F_m is the frequency of the modulating signal (voice)

Using only the first order sidebands, the bandwidth requirement is

$$1.25 \text{ Mc} + \frac{21 \text{ kc}}{2} = 2.521 \text{ Mc}$$

This is the reason for the 3.3 Mc bandwidth in the receiver. Figure 7 shows the USB frequency spectrum.

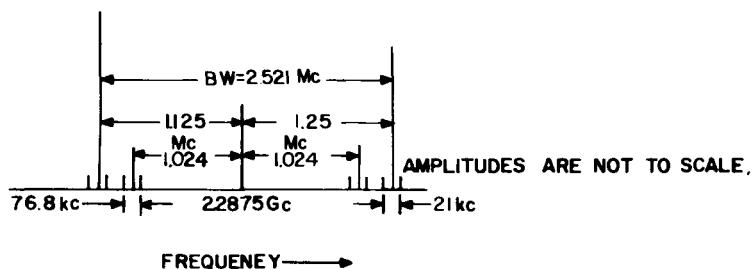


Figure 7. USB Frequency Spectrum

The data demodulator now must extract the signal from the subcarrier. The TLM signal is PCM/PM (biphase) modulated at $PSK \pm 90^\circ$ (1.57 radians) for the 51.2-kbps data rate.

To obtain alternate "zero" and "one" bits the baseband bandwidth should be:

$$BW = \frac{3}{4 \times \text{Bit Period}} = \frac{3 \times 10^3}{4 \times .0195} = 38.4 \text{ kc}$$

$$\text{where: Bit Period} = \frac{1}{\text{Bit Rate}} = \frac{1}{51.2\text{K}} = .0195 \times 10^{-3}$$

$$\text{Modulation Bandwidth} = BW_m = 2(\Delta F = BW)$$

$$BW_m = 2(0 + 38.4) = 76.8 \text{ kc}$$

Using a biphase modulation index, $\Delta\theta$, of 1.57 radians ($\frac{\pi}{2}$) causes operation outside of the linear region of the A/RIA data demodulator. To reduce the voltage response from the linear value, use the factor:

$$\frac{\sin \Delta\theta}{\Delta\theta} = \frac{\sin \pi/2}{\pi/2} = \frac{1}{1.57}$$

The biphasic modulation with this index will give a peak response equivalent to that for a $\Delta\theta^2 = \frac{1.57}{1.57} = 1$ radian peak swing for a linear detector. The rms value of this is .707. However, phase jitter (or noise) = σ (radians) = $1/\sqrt{2} \frac{S}{N_1}$ or $\sigma^2 = \frac{1}{2(S/N)_o}$ where $(S/N)_o$ is the postdetection S/N.

With a reasonable amount of phase jitter in the data demodulator (less than .35 radians), the loss due to modulation becomes:

$$\left(\frac{S}{N}\right)_o = \frac{1}{2\sigma^2} = \frac{1}{2(.35)^2} = \frac{1}{2(.1225)} = 4.09$$

$$\text{db loss} = 10 \log 4.09 = 10 (.611) = -6.11 \text{ db}$$

Combining the effects of bandwidth and modulation, the overall effect is $+4.09 - 6.11 = -2.02$ db.

If the equation for reference 1 were used directly,

$$\frac{S}{N}_{\text{out}} = \frac{(0.707)^2}{1} \cdot \frac{B}{2b} = \frac{B}{2b} \cdot \left(\frac{S}{N}\right)_{\text{in}}$$

where: B = predetection bandwidth*

b = postdetection bandwidth*

* Where both are noise bandwidths and not signal bandwidths.

$$\text{In decibels this is: } \left(\frac{S}{N}\right)_{\text{out, db}} = 10 \log \left(\frac{S}{N}\right)_o = 10 \log \frac{B}{2b} - 10 \log \left(\frac{S}{N}\right)_{\text{in}}$$

where: $(S/N)_1$ = the per cycle bandwidth for the predetection position

$$\left(\frac{S}{N}\right)_o \text{ db} = 10 \log \frac{1}{2(90)} + \left(\frac{S}{N}\right)_i \text{ db} = \left(\frac{S}{N}\right)_i \text{ db} - 10 \log 180,000$$

$$\left(\frac{S}{N}\right)_o \text{ db} = \left(\frac{S}{N}\right)_i \text{ db} - 10(5.255) = \left(\frac{S}{N}\right)_i \text{ db} - 52.55$$

In this paper, the received predetection signal power was found to be 134.6 db/cycle (table 2). The noise spectral density was calculated at 201.24 db. (Some reduction in this is possible since two receivers may be used, thus changing the receiver losses.) This leaves a $(S/N)_i$ db of +66.64/cycle bandwidth. Using the predetection bandwidth of 462 kc a db value of $10 \log 462,000 = 10 (5.665) = 56.65$ db, the predetection S/N is +10 db. This is the value shown in table 2.

Now, using the predetection bandwidth, several possibilities present themselves for determining the postdetection $(S/N)_o$. First,

$$\left(\frac{S}{N}\right)_o \text{ db} = \left(\frac{S}{N}\right)_i \text{ db} - 52.55 = 66.64 - 52.55 = 14.09 \text{ db}$$

but there is considerable doubt about this equation. Secondly, the predetection S/N of +10 db can be used and combined with the composite of modulation index and bandwidth improvement through the demodulator of -2 db to obtain a postdetection S/N of +8 db. This is the value used in table 2.

3.3.2.12 S/N for 10^{-4} Bit Error Probability

Using reference 1, the following deviation is found. The bit error probability is a function of the normalized SNR, E/N_o , where: E = Average signal energy per bit

N_o = Noise power density

The average SNR, S/N, is related to the normalized SNR by the equation

$$S/N = \frac{E/T_o}{N_o b} = \frac{E}{N_o} \frac{1}{T_o b}$$

where: T_o = bit duration, and b = postdetection bandwidth since,
 $1/T_o$ = bit frequency = f_b

$$\text{then } S/N = \frac{E}{N_o} \cdot \frac{f_b}{b}$$

$$\text{In decimal form } \left(\frac{S}{N}\right)_{\text{db}} = \frac{E}{N_o} \text{ db} = 10 \log \frac{f_b}{b}$$

The required value of $\left(\frac{E}{N_o}\right)_{\text{db}}$ for a bit error probability of 10^{-4} in a differentially coherent PSK system is found to be 9.2 db.

$$\text{Then: } \left(\frac{S}{N}\right)_{\text{db}} = 9.2 + 10 \log \frac{f_b}{b}$$

For the bit frequency of 51.2 kbps, $b = 75 \text{ kc}$, and $\left(\frac{S}{N}\right)_{\text{db}} = 9.2 + 10 \log \frac{51.2}{75} = 9.2 + 10 \log .683 = 9.2 - 1.6 = +7.6 \text{ db}$

3.3.2.13 Receiver Measurements. Prior to the departure of NASA 432 from the GSFC area, the receivers, tracking, and data were tested against a test aircraft in Quincy, Mass. The results were:

- a. Measured full power, carrier and sideband, required for acceptable antenna tracking was -116 dbm (-146.0 dbw), table 1.
- b. Measured total power level for acceptable data recording -102 to -106 db. Using the -102-db figure, the data signal level is 14 db below the tracking signal level. This is the same value arrived at analytically.

3.3.3 TIME VARIABLE VALUES

3.3.3.1 General. As the spacecraft moves along its flight path, three losses vary greatly. First, the point on the spacecraft "viewed" from the aircraft changes causing a variation in the transmitting antenna's gain since it is not a perfect omnidirectional antenna. Secondly, the slant range, spacecraft to aircraft varies which causes a change in the space loss. Third, the reflection of the signal from the earth (water) causes two signals to arrive at the antenna at the same time. This will reduce the effective signal, and it is referred to as multipath.

3.3.3.2 Transmitting Antenna Gain (G_t)

Gain of the CSM omnidirectional antenna is -3 db according to Block I performance and interface specification revisions. This could be modified by the data on the propagation curves. It is expected that this could be as great as -15 db. The most likely value would be -3 db; however, figure 8 shows the variation in G_t vs time.

The greatest difficulty in this area was the determination of the proper angles used on the propagation curve (see figure 9). Figure 10 shows the coordinate system used and figure 11 shows the physical location of the antennas. For re-entry conditions in the AS-202 mission, the surviving antenna is used (AS-1). The angles used on the propagation curve are θ and ϕ , and they are defined as:

$$\phi = \tan^{-1}\left(\frac{Y_1}{-Z_1}\right) = \tan^{-1}\left(\frac{Y_b}{-Z_b}\right)$$

$$\theta = \tan^{-1}\left(\frac{-Z_1}{X_1}\right) = \tan^{-1}\left(\frac{-Z_b}{-X_b}\right)$$

$$\text{where: } X_1 = -X_b$$

$$Y_1 = -Y_b$$

$$Z_1 = Z_b$$

and "1" subscripts are for launch or earth coordinates and "b" subscripts are for re-entry coordinates. Figure 12 shows the spacecraft in the re-entry attitude and is the vector diagram for the spacecraft position at 80 seconds after entry.

3.3.3.3 Space Loss (L_s)

If a point source of radiated power, P_t , is assumed (omnidirectional antenna), and if this power is transmitted from an antenna of gain G_t , and if the aircraft antenna having an effective area A is located at a distance R ; the power received (ref. figure 13), P_r , is:

$$P_r = \frac{P_t G_t A}{4\pi R^2}$$

where: $4\pi R^2$ is the area of a sphere.

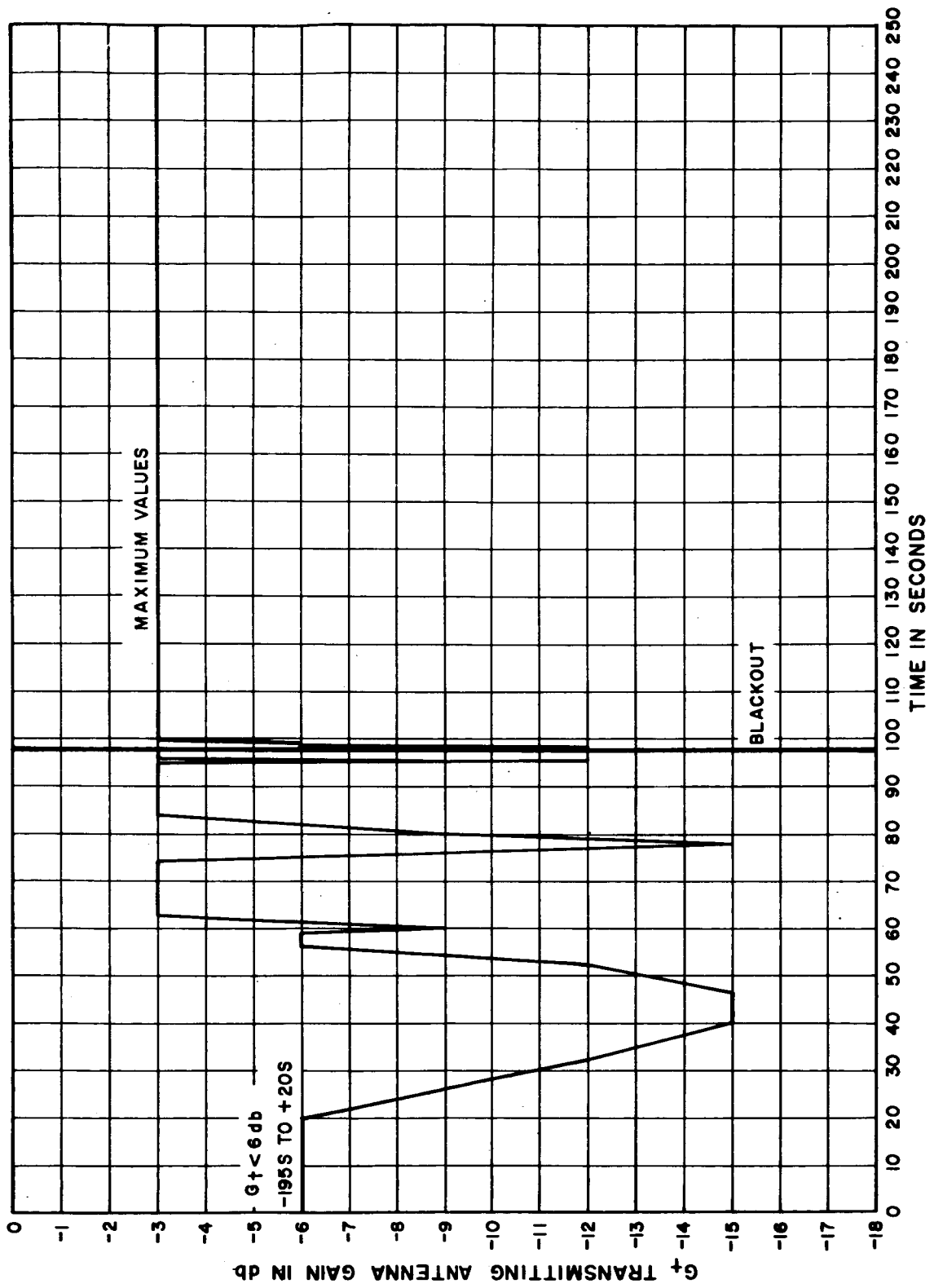
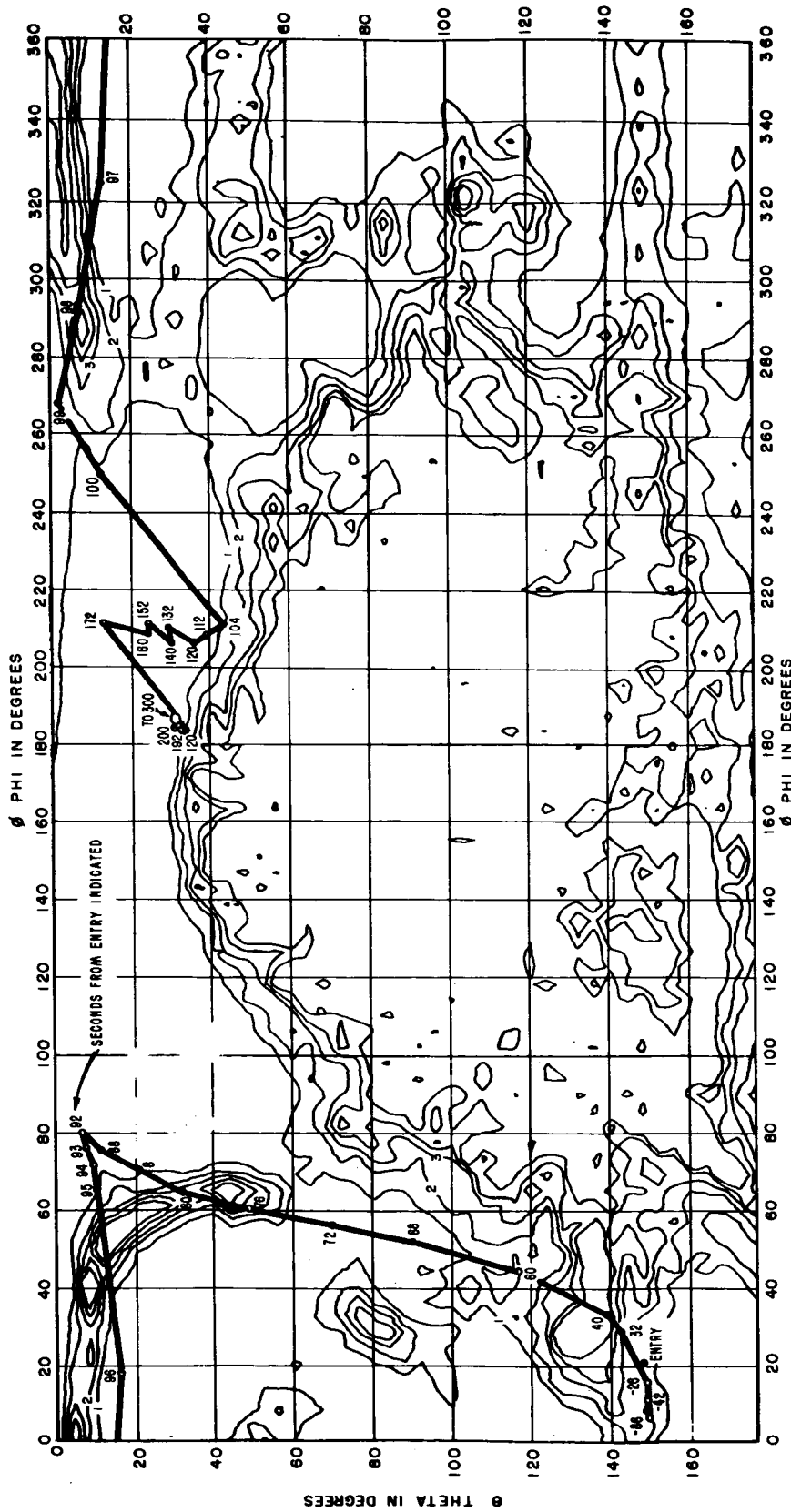


Figure 8. AS-202/NASA 432 USB Downlink Transmitting
Antenna Gain vs Time



* 0 db REFERENCE LEVEL FOR CONTOUR IS THE LEVEL THAT WOULD BE PROVIDED BY A LOSSLESS ISOTROPIC ANTENNA WHEN ILLUMINATED WITH A CIRCULARLY POLARIZED PLANE WAVE.

PATTERN OF TEST VEHICLE	23103 APOLLO	TRANS. POL.	RCP	LEVELS(K)	* -3K db LEVEL	INDIV. COVG. FACTORS	COMB. COVG. FACTORS
ANTENNA TYPE	CM W/UMB. SURV. SCIN. ON CM W/ ABLATOR	TRANS. ELLIP. DIRECTIVITY OF/BOTH RCP & LCP	1.3 db 8.2 db	1 2 3 4 5 6 7	-3 db -6 -9 -12 -15 -18 -21	32.0% 10.6 7.7 7.0 6.7 10.1 9.6	32.0% 42.6 50.3 57.3 66.0 76.1 86.7
MODEL SCALE	1/3	EFFICIENCY	-3.0 db				
FULL SCALE FREQUENCY	2287.5 MHZ						

Figure 9. Propagation Plot of Apollo CM Model

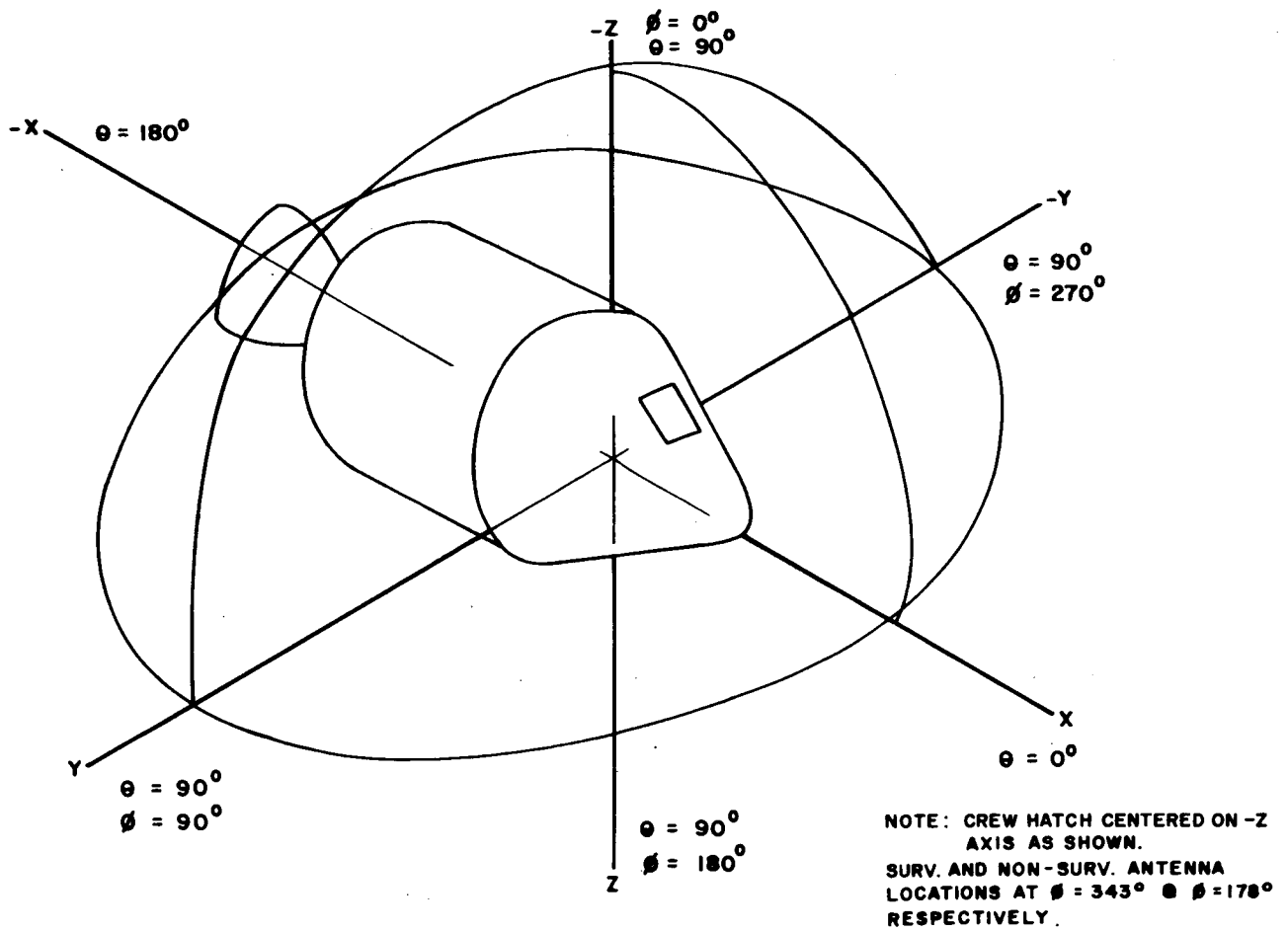


Figure 10. Coordinate System (See Reference 9)

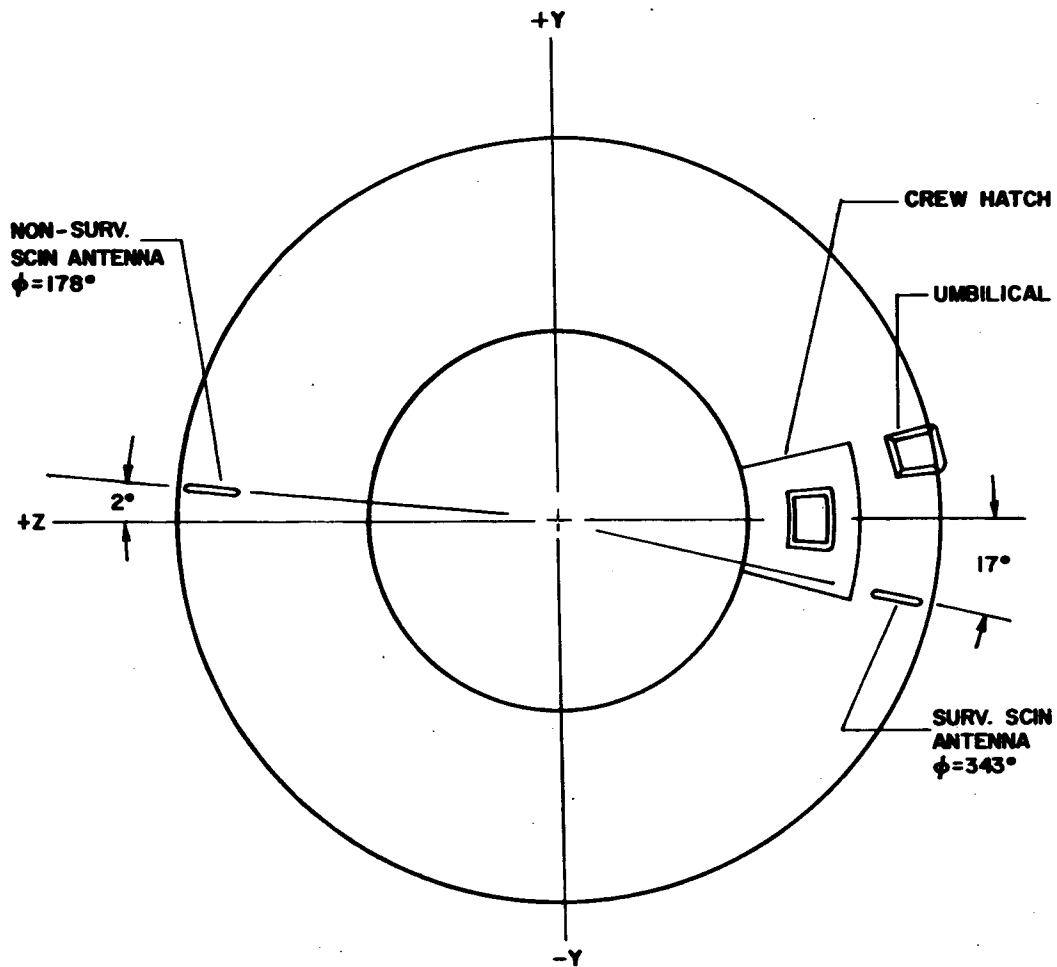
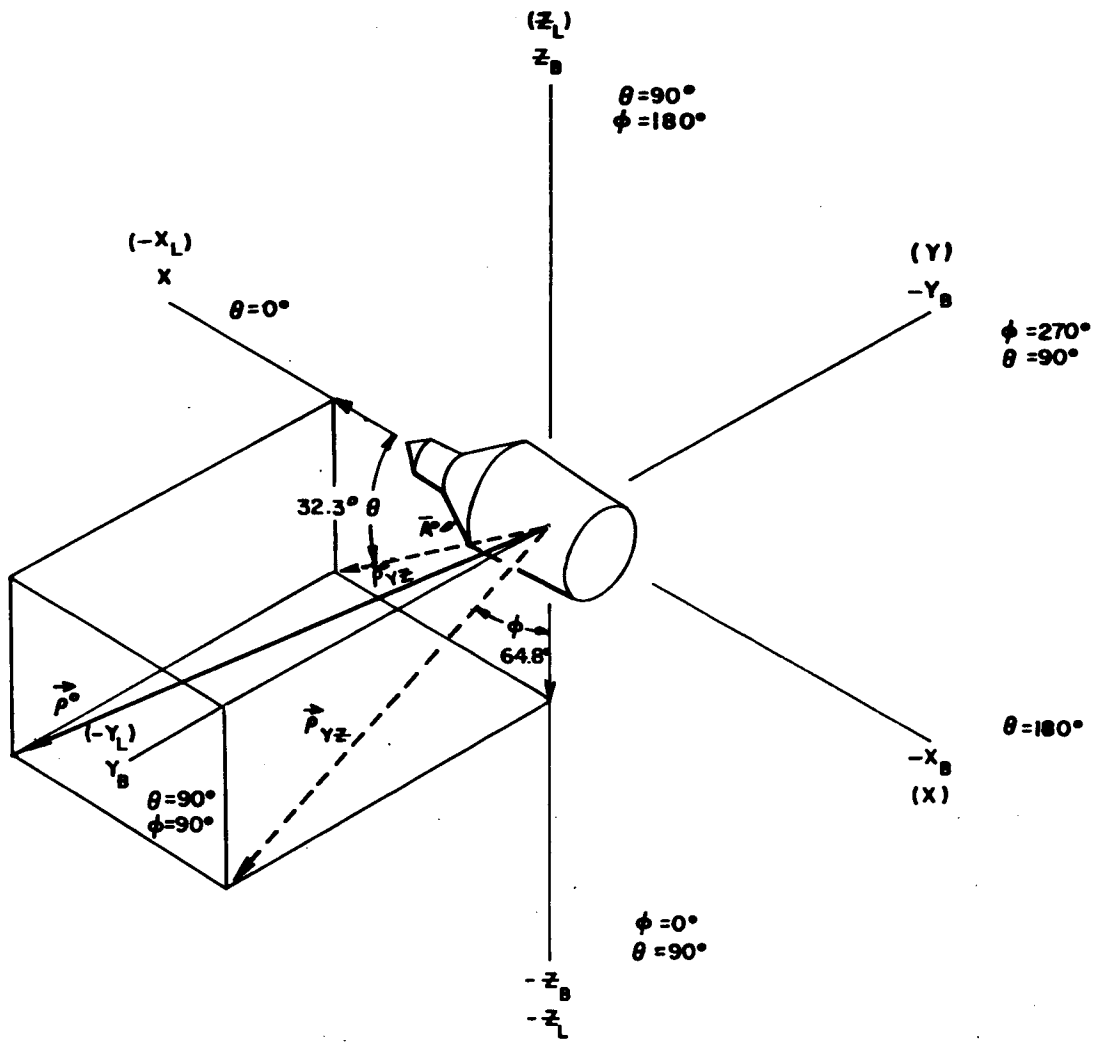


Figure 11. Apollo SCIN Antenna Locations (View Looking Aft)



LEGEND:
 LAUNCH COORDINATES X_L, Y_L, Z_L
 VEHICLE COORDINATES X, Y, Z

Figure 12. Spacecraft Coordinates in Reentry Attitude at Position 80 Seconds After Entry

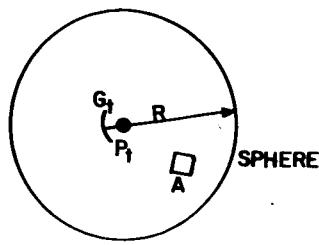


Figure 13. Space Loss

From antenna theory, the gain of a directional antenna (receiving) G_r , as a function of effective area, A , is:

$$G_r = \frac{4\pi A}{\lambda^2} ,$$

$$\text{or } A = \frac{G_r \lambda^2}{4\pi}$$

Now the received power is:

$$P_r = \frac{P_t G_t G_r \lambda^2}{(4\pi R)^2}$$

where: $\lambda^2 / (4\pi R)^2$ is defined as the space loss, L_s .

and since $\lambda = c/f$

$$L_s = \left(\frac{C}{4\pi R f} \right)^2$$

where: $C = 186,272$ miles/sec

or $C = 186,272 \cdot \frac{5280}{6080} = 162,000$ nmi/sec

and $R = 500$ nmi

$f = 2.2875$ Gc

Putting this into dbw gives:

$$L_s = 20 \log \frac{C (X10^6 \text{ nmi/sec})}{4\pi R f \text{ Mc}} =$$

$$L_s = -20 \log \frac{4\pi}{.162} -20 \log 500 -20 \log 2287.5$$

$$L_s = -20 \log 77.5 -20 \log 500 -20 \log 2287.5$$

$$L_s = -20 (1.889) -20 (2.698) -20 (3.359)$$

$$L_s = -37.78 -53.96 -67.18$$

$$L_s = -158.92$$

Since space loss varies with range, and since it is one of the largest variables in the margin calculations, it is plotted vs range for the determination of data margins in figure 14.

4. FUTURE WORK

Although the obtainment of signal margins has been done many times, there is a great deal of work required in the area of determining margins for telemetry systems, particularly when these are incorporated into a larger system as is done in the USB. With the different techniques used in demodulating and also tracking a signal, these areas also grow in difficulty when applied to the USB. In short, further work is needed to develop accurate techniques for predicting signal strengths in the multiple signal systems in the tracking and data reception modes.

5. ACKNOWLEDGEMENTS

This report is a direct result of the ASEE-NASA Summer Faculty Fellowship Program. It is also the result of having the stimulating experience of working directly on a project that relates to an imminent space mission. The author extends his thanks to Mr. David J. Graham, his Research Colleague of the Manned Flight Operations Branch, who patiently guided his studies; to Mr. Daniel Spintman, who kept him on course; and to the many others in the Branch, without whose assistance the program would not have been successful.

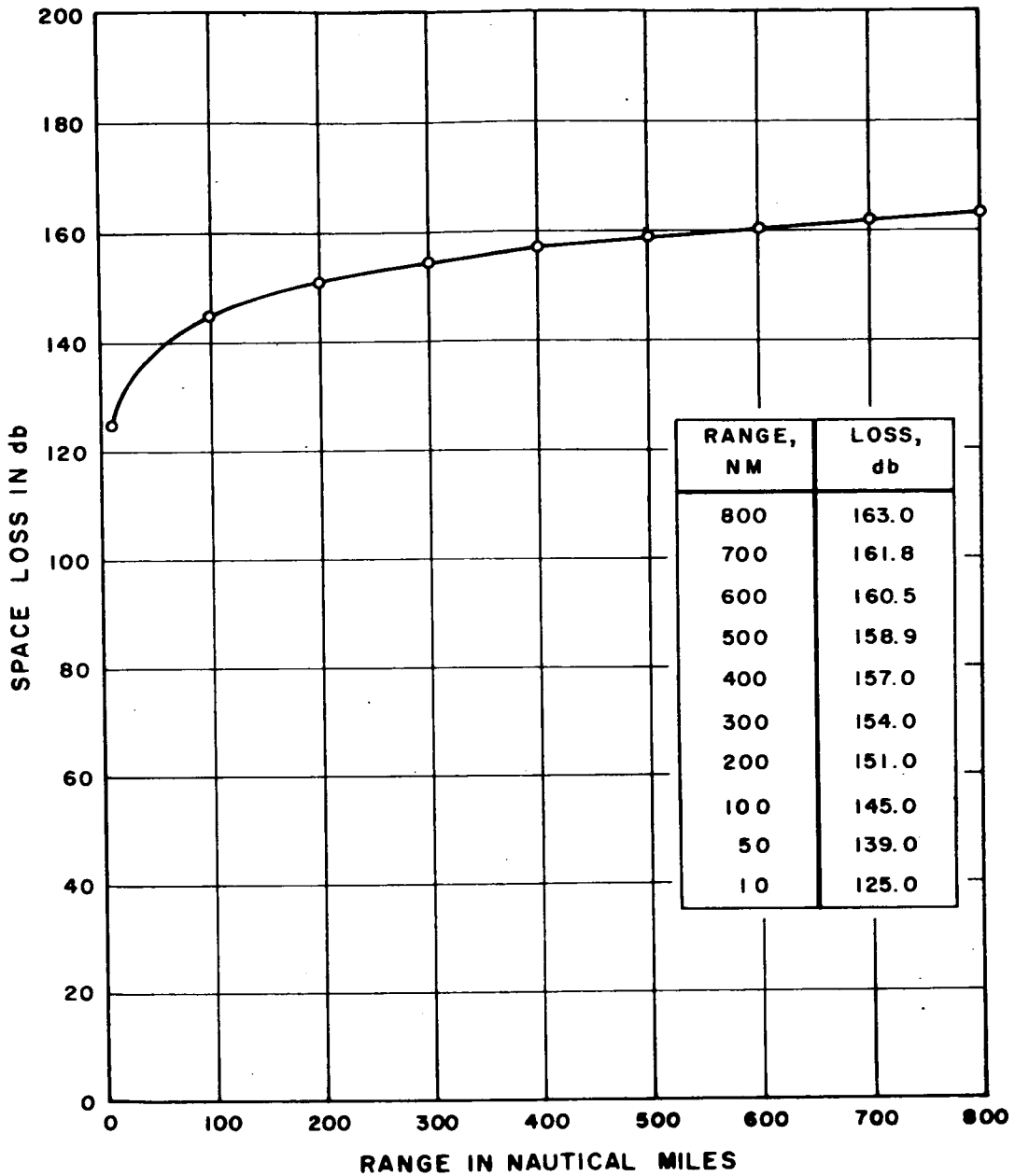


Figure 14. Space Losses at 2287.5 Mc

6. REFERENCES

1. "Revised Calculations of Margins for CSM Unified S-Band Downlink Channel" by G. Soukup and M. Taylor, Bendix Corporation A/RIA Technical Note A0141, May 20, 1966.
2. "Mathematical Relationships of Carrier Power and Subcarrier Powers in Frequency and Phase Modulated Signals," by R. C. Walch, Jr., Bendix Corporation A/RIA Technical Note 0002, April 15, 1965.
3. "The Effective Noise Temperature of the Sky" by David C. Hogg and W. W. Mumford, Microwave Journal, March 1960.
4. Antenna Engineering Handbook, Henry Jaskik, Ed., McGraw-Hill Book Company, Inc., New York, 1961.
5. Introduction to Radar Systems, Merrill I. Skolnik, McGraw-Hill Book Company, Inc., New York, 1962.
6. "Link Parameters for Apollo Missions," by G. Soukup and M. Taylor, Bendix Corporation A/RIA Technical Note A0137, March 23, 1966.
7. "A/RIA Meeting Notes", D. J. Graham, et.al., GSFC, April 12, 1966 (Unpublished).
8. "Re-entry Aircraft Test Plan for the Apollo AS-202", by J. R. Moore and F. O. Vonbun, Unpublished Report, August 6, 1966
9. Memorandum: PF/Apollo Configuration Control, February 1, 1966.